Ground-state baryon masses in the perturbative chiral quark model

T. Inoue, V. E. Lyubovitskij, Th. Gutsche and Amand Faessler

Institut für Theoretische Physik, Universität Tübingen, Auf der Morgenstelle 14, D-72076 Tübingen, Germany

Abstract

Mass differences of the flavor octet and decuplet ground-state baryons are studied in the perturbative chiral quark model. We present a way to understand the nontrivial spin- and flavor dependent mass differences, where both pseudoscalar mesons and gluons play a significant role.

PACS: 12.39.Ki, 12.40.Yx, 14.20.Dh, 14.20.Gk

Keywords: Chiral symmetry; Relativistic quark model; Effective Lagrangian; Baryon mass shifts.

I. INTRODUCTION

In the naïve non-interacting quark model the masses of ground-state baryons are solely classified by their strangeness. Therefore, in this limit the masses of nucleon and Δ, and also that of Λ and Σ, are degenerate. Traditionally, this degeneracy is removed by introducing a hyperfine(spin-spin) interaction [1,2]

$$H_{\rm hyp} = \frac{1}{2} \sum_{i<j} \mathcal{H}_{ij}\, \vec{s}_i \cdot \vec{s}_j\, \delta^3(\vec{r}_i - \vec{r}_j) \tag{1}$$

where $\vec{s}_i$ is the spin operator acting on the i-th quark. Here, $\mathcal{H}_{ij}$ is the two-body quark coupling which includes a common color factor $-2/3$ and explicitly depends on the flavor of the constituent quarks through their masses m_i and m_j:

$$\mathcal{H}_{ij} \sim \frac{2}{3} \frac{1}{m_i\, m_j}\,. \tag{2}$$

The use of $SU(6)$ spin-flavor wave functions for the ground-state baryons B leads to simple relations between the matrix elements $\langle B|\, H_{\rm hyp}\, |B\rangle$, which are the perturbative mass shifts due to the hyperfine interaction. Denoting the contribution from a non-strange quark pair as $\mathcal{H}_{qq}$ (and similarly for strange quarks with q replaced by s), in the isospin limit the masses of the ground-state baryons are composed as [2]

$$
\begin{array}{ll}
m_N = 3E_0 - \frac{3}{8}\mathcal{H}_{qq} & m_\Delta \;= 3E_0 + \frac{3}{8}\mathcal{H}_{qq} \\
m_\Lambda = 2E_0 + E_0^s - \frac{3}{8}\mathcal{H}_{qq} & m_{\Sigma^*} = 2E_0 + E_0^s + \frac{1}{8}\mathcal{H}_{qq} + \frac{1}{4}\mathcal{H}_{qs} \\
m_\Sigma = 2E_0 + E_0^s + \frac{1}{8}\mathcal{H}_{qq} - \frac{1}{2}\mathcal{H}_{qs} & m_{\Xi^*} = E_0 + 2E_0^s + \frac{1}{4}\mathcal{H}_{qs} + \frac{1}{8}\mathcal{H}_{ss} \\
m_\Xi = E_0 + 2E_0^s - \frac{1}{2}\mathcal{H}_{qs} + \frac{1}{8}\mathcal{H}_{ss} & m_\Omega \;= 3E_0^s + \frac{3}{8}\mathcal{H}_{ss}
\end{array}
\tag{3}
$$

Here, E_0 and E_0^s are the single particle ground-state energies of the non-strange and strange quark, respectively. These mass formulas satisfy the Gell-Mann-Okubo mass relations

$$
m_\Sigma - m_N = \frac{1}{2}(m_\Xi - m_N) + \frac{3}{4}(m_\Sigma - m_\Lambda)\,, \quad m_{\Sigma^*} - m_\Delta = m_{\Xi^*} - m_{\Sigma^*} = m_\Omega - m_{\Xi^*} \tag{4}
$$

providing a condition on the matrix elements of the residual interaction with $\mathcal{H}_{qq} - \mathcal{H}_{qs} \simeq \mathcal{H}_{qs} - \mathcal{H}_{ss}$. With the choice $E_0^s - E_0 \simeq 180$ MeV, $\mathcal{H}_{qq} \simeq 400$ MeV and $\mathcal{H}_{qq} - \mathcal{H}_{qs} \simeq \mathcal{H}_{qs} - \mathcal{H}_{ss} \simeq 150$ MeV, all the observed mass differences can be roughly reproduced.

The hyperfine interaction of Eq. (1) can for example be generated by the one-gluon-exchange mechanism between two quarks (in the non-relativistic reduction) [3]. Actually, the relevant part for the ground-state baryons is just given by the form of Eq. (1), and the mass differences in the multiplet have been explained [3]. Moreover, mass and structure of excited p-wave baryons have been studied successfully by taking into account the hyperfine interaction including a tensor term involved in the one-gluon-exchange [4].

During the last decade quark models based on one-meson-exchange responsible for the inter-quark forces are often used as an alternative to study the baryon mass spectrum and various consequences resulting from the structure of these states [5–13]. The relevant short range part of the force is essentially the hyperfine interaction of the form $\vec{\lambda}_i \cdot \vec{\lambda}_j \; \vec{s}_i \cdot \vec{s}_j \; \delta^3(\vec{r}_i - \vec{r}_j)$, where an explicit flavor dependence is implemented by the flavor operators $\vec{\lambda}$, and hence in its flavor dependence is different from Eq. (1). In these works the baryon spectrum including the splitting within flavor multiplets, is quantitatively explained by this force instead of Eq. (1), when adjusting the radial dependence of the interaction phenomenologically. Both of these two mechanisms for explaining the flavor and spin dependence of baryon masses are based on the non-relativistic picture with massive constituent quarks.

The importance of chiral symmetry for the phenomenology of hadron physics at low and intermediate energies has been worked out and strongly established. The spontaneous breakdown of chiral symmetry leads to the presence of Goldstone bosons, which are realized by the low-lying octet of pseudoscalar mesons. Therefore, it is natural to expect that the Goldstone bosons play a significant role in the description of the spectrum of baryons and their structure. However, other mechanisms, such as one-gluon exchange, still can play some role.

The Graz group [7] claims that a possible gluon-exchange is excluded in their quark model which is solely based on Goldstone dynamics, while the Salamanca-Valencia approach [9] resorts to a strong residual gluon interaction. In both works the key justification for the respective flavor- and spin-dependent quark interactions rests on the correct description of the level ordering in the nucleon spectrum, *i.e.* the positive parity Roper resonance (1440) moves below the negative parity N^* (1535) by the effect of the residual interaction. Actually, results and conclusions drawn strongly depend on the treatment of the kinetic term (*i.e.* non-, semi-, or full-relativistic) and of the short-range interaction (contact term or smeared out interaction) [12]. In addition, in the quark model approach it is assumed that resonances are exclusively described as simple excited three quark systems.

Dynamical generation of resonances in multichannel approaches are an alternative picture to possibly explain the excitation spectrum of baryons. For example, in the chiral unitary approach, the $N^*(1535)$ resonance is mainly a $K\Sigma$ and $K\Lambda$ system [14–17]. This approach suggests that the coupling to configurations by creating a $s\bar{s}$ pair is essential to explain the resonance structure in the quark picture. Also, an even more complicated multi-channel structure is seemingly underlying the Roper resonance [18–21].

In this paper we study the mass spectrum of the so-called ground-state baryons in a relativistic chiral quark model. Here we restrict to the octet and decuplet ground states of flavor SU(3) baryons, since the valence quark component is the leading contribution and the residual interaction can be treated perturbatively.

The perturbative chiral quark model [22–25] is an effective model of baryons based on chiral symmetry. The baryon is described as a state of three localized relativistic quarks supplemented by a pseudoscalar meson cloud as dictated by chiral symmetry requirements. In this model the effect of the meson cloud is evaluated perturbatively in a systematic fashion. The model has been successfully applied to the nucleon electro-magnetic form factors, the meson-nucleon sigma term, the nucleon-Δ photo-transition and the nucleon axial coupling constant amongst other applications. In this paper, we extend the model to include gluon degrees of freedom and we also introduce a violation of flavor $SU(3)$ symmetry. Then we evaluate meson and gluon cloud induced mass shifts for the octet and decuplet of ground-state baryons.

This paper is organized as follows. In Section II, we introduce the perturbative chiral quark model with additional gluon degrees of freedom and the flavor violation. In Section III, we study the masses of the ground-state baryon within the model. Section IV contains a summary of our major conclusions.

II. THE PERTURBATIVE CHIRAL QUARK MODEL (PCQM)

The perturbative chiral quark model [22–25] is based on an effective chiral Lagrangian describing the valence quarks of baryons as relativistic fermions moving in an external field (static potential) $V_{\rm eff}(r) = S(r) + \gamma^0 V(r)$ with $r = |\vec{x}|$ [22,23], which in the $SU(3)$-flavor version are supplemented by a cloud of Goldstone bosons (π, K, η). The origin of a such an effective potential can be phenomenologically understood by the assumptions of Refs. [26] where the gluon field can be decomposed into the vacuum background configuration and small quantum fluctuations around it. In particular, the vacuum component of the gluon field provides the confinement of quarks, which in turn is encoded in a confinement potential. The quantum fluctuations of the gluon field can be also taken into account by dressing the quark fields using a perturbative expansion.

When treating Goldstone fields and the quantum components of the gluon fields as small fluctuations around the three-quark (3q) core, we have the linearized effective Lagrangian [22,23]:

$$\mathcal{L}_{\rm eff}(x) = \bar{\psi}(x)[i\ \partial\!\!\!/ - V_{\rm eff}(r)]\psi(x) + \frac{1}{2}\sum_{i=1}^{8}[\partial_\mu \Phi_i(x)]^2 - \frac{1}{4}F^a_{\mu\nu}F^{a\,\mu\nu}$$
$$- \bar{\psi}(x)\Big\{ S(r) i\gamma^5 \frac{\hat{\Phi}(x)}{F} + g_s \gamma^\mu A^a_\mu(x)\frac{\lambda^a}{2}\Big\}\psi(x) + \mathcal{L}_{SB}(x). \qquad (5)$$

$F = 88$ MeV is the pion decay constant in the chiral limit [27]; g_s is the quark-gluon coupling constant; A^a_μ is the quantum component of the gluon field and $F^a_{\mu\nu}$ is its conventional field strength tensor; $\hat{\Phi} = \sum_{i=1}^{8} \Phi_i \lambda_i = \sum_P \Phi_P \lambda_P$ is the octet matrix of pseudoscalar mesons with $P = \pi^\pm, \pi^0, K^\pm, K^0, \bar{K}^0, \eta$. The explicit relations between the sets $\{\Phi_P, \lambda_P\}$ and $\{\Phi_i, \lambda_i\}$ are given in Ref. [25].

The term $\mathcal{L}_{SB} = \mathcal{L}_{\chi SB} + \bar{\mathcal{L}}_{SB}$ in Eq. (5) contains the mass contributions $\mathcal{L}_{\chi SB}$ both for quarks and mesons, which explicitly break chiral symmetry,

$$\mathcal{L}_{\chi SB}(x) = -\bar{\psi}(x)\mathcal{M}\psi(x) - \frac{B}{2} Tr[\hat{\Phi}^2(x)\mathcal{M}]\,, \tag{6}$$

and the term $\bar{\mathcal{L}}_{SB}$, which breaks the unitary flavor $SU(3)$ symmetry:

$$\bar{\mathcal{L}}_{SB}(x) = -\bar{\psi}(x)\Delta V_{\rm eff}(r)\lambda_s\psi(x)\,. \tag{7}$$

Here, $\mathcal{M} = \mathrm{diag}\{m_u, m_d, m_s\}$ is the mass matrix of current quarks, $B = -\langle 0|\bar{u}u|0\rangle/F^2$ is the quark condensate constant, $\Delta V_{\rm eff}(r) = \Delta S(r) + \gamma^0 \Delta V(r)$ is a correction to the confinement potential for strange quarks and $\lambda_s = \mathrm{diag}\{0, 0, 1\}$ is the strangeness matrix. We suppose that the nonstrange and the strange quarks are exposed to a different confinement and, therefore, introduce flavor dependent phenomenological potentials: $V_{\rm eff}(r)$ for nonstrange quarks and $V_{\rm eff}(r) + \Delta V_{\rm eff}(r)$ for the strange quark. In practice, it is convenient to separate the term

$$\bar{s}\Delta V_{\rm eff}(r)s = \bar{\psi}\Delta V_{\rm eff}(r)\lambda_s\psi$$

and treat it as an operator which breaks the flavor $SU(3)$ symmetry. After diagonalization the meson mass terms take the form

$$\frac{B}{2}\,\mathrm{Tr}[\hat{\Phi}^2(x)\mathcal{M}] = \frac{1}{2}\sum_P M_P^2\,\Phi_P^2(x) \tag{8}$$

where M_P is the set of pseudoscalar meson masses. In the numerical calculations we restrict to the isospin symmetry limit with $m_u = m_d = \hat{m}$. We rely on the standard picture of chiral symmetry breaking [28] and for the masses of pseudoscalar mesons we use the leading term in their chiral expansion, i.e. linear in the current quark masses (see exact expressions in Ref. [25]. In the isospin limit they are given by

$$M_\pi^2 = 2\hat{m}B, \quad M_K^2 = (\hat{m} + m_s)B, \quad M_\eta^2 = \frac{2}{3}(\hat{m} + 2m_s)B. \tag{9}$$

The following set of parameters [28] is chosen in our evaluation

$$\hat{m} = 7\ \mathrm{MeV},\ \frac{m_s}{\hat{m}} = 25,\ B = \frac{M_{\pi^+}^2}{2\hat{m}} = 1.4\ \mathrm{GeV}. \tag{10}$$

Meson masses obtained by Eq. (9) satisfy the Gell-Mann-Oakes-Renner and the Gell-Mann-Okubo relation. In addition, the linearized effective Lagrangian in Eq. (5) fulfills the PCAC requirement.

We expand the quark field ψ in the basis of potential eigenstates as

$$\psi(x) = \sum_\alpha b_\alpha u_\alpha(\vec{x}) \exp(-i\mathcal{E}_\alpha t) + \sum_\beta d_\beta^\dagger v_\beta(\vec{x}) \exp(i\mathcal{E}_\beta t)\,, \tag{11}$$

where the sets of quark $\{u_\alpha\}$ and antiquark $\{v_\beta\}$ wave functions in orbits α and β are solutions of the Dirac equation with the static potential $V_{\rm eff}(r) + \Delta V_{\rm eff}(r)\lambda_s$. The expansion coefficients b_α and $d_\beta^\dagger$ are the corresponding single quark annihilation and antiquark creation operators.

We formulate perturbation theory in the expansion parameter $\hat{\Phi}(x)/F \sim 1/\sqrt{N_c}$ and treat finite current quark masses perturbatively [22]. All calculations are performed at one loop or at order of accuracy $o(1/F^2, \hat{m}, m_s)$. In the calculation of matrix elements we project quark diagrams on the respective baryon states. The baryon states are conventionally set up by the product of the $SU(6)$ spin-flavor and $SU(3)_c$ color wave functions. Then the nonrelativistic single quark spin wave function is replaced by the relativistic solution $u_\alpha(\vec{x})$ of the Dirac equation

$$\Big[-i\gamma^0\vec{\gamma}\cdot\vec{\nabla} + \gamma^0 S(r) + V(r) - \mathcal{E}_\alpha^q\Big]\, u_\alpha^q(\vec{x}) = 0 \tag{12}$$

for nonstrange quarks, and

$$\Big[-i\gamma^0\vec{\gamma}\cdot\vec{\nabla} + \gamma^0\{S(r) + \Delta S(r)\} + V(r) + \Delta V(r) - \mathcal{E}_\alpha^s\Big]\, u_\alpha^s(\vec{x}) = 0 \tag{13}$$

for the strange quark. Here, index q refers to the nonstrange (u or d) whereas s to the strange quark; $\{u_\alpha^q, \mathcal{E}_\alpha^q\}$ and $\{u_\alpha^s, \mathcal{E}_\alpha^s\}$ are the single-quark wave functions and energies of nonstrange and strange quark, respectively.

For the description of baryon properties on tree level we use the effective potentials $V_{\rm eff}(r)$ and $\Delta V_{\rm eff}(r)$ with a quadratic radial dependence [22,23]:

$$S(r) = M_1 + c_1 r^2, \qquad V(r) = M_2 + c_2 r^2 \tag{14}$$

$$\Delta S(r) = \Delta M_1 + \Delta c_1 r^2, \qquad \Delta V(r) = \Delta M_2 + \Delta c_2 r^2 \tag{15}$$

with the particular choice

$$M_1 = \frac{1\,-\,3\rho_q^2}{2\,\rho_q R_q}, \qquad M_2 = \mathcal{E}_0^q - \frac{1\,+\,3\rho_q^2}{2\,\rho_q\,R_q}\,, \qquad c_1 \equiv c_2 = \frac{\rho_q}{2R_q^3}\,, \tag{16}$$

$$M_1 + \Delta M_1 = \frac{1\,-\,3\rho_s^2}{2\,\rho_s\,R_s}\,, \quad M_2 + \Delta M_2 = \mathcal{E}_0^s - \frac{1\,+\,3\rho_s^2}{2\,\rho_s\,R_s}, \quad c_1 + \Delta c_1 \equiv c_2 + \Delta c_2 = \frac{\rho_s}{2R_s^3}\,. \tag{17}$$

Here, the potential parameters are related to the set of quantities (R_q, ρ_q) and (R_s, ρ_s), which characterize the ground-state wave function of nonstrange (u_0^q) and strange quark (u_0^s):

$$u_0^q(\vec{x}) \;=\; N_q\, \exp\Big[-\frac{\vec{x}^{\,2}}{2R_q^2}\Big] \begin{pmatrix} 1 \\ i\rho_q\,\vec{\sigma}\vec{x}/R_q \end{pmatrix} \chi_s\,\chi_f\,\chi_c\,, \tag{18}$$

$$u_0^s(\vec{x}) \;=\; N_s\, \exp\Big[-\frac{\vec{x}^{\,2}}{2R_s^2}\Big] \begin{pmatrix} 1 \\ i\rho_s\,\vec{\sigma}\vec{x}/R_s \end{pmatrix} \chi_s\,\chi_f\,\chi_c, \tag{19}$$

where $N_q = [\pi^{3/2}R_q^3(1+3\rho_q^2/2)]^{-1/2}$ and $N_s = [\pi^{3/2}R_s^3(1+3\rho_s^2/2)]^{-1/2}$ are the corresponding normalization constants; χ_s, χ_f, χ_c are the spin, flavor and color quark wave functions,

respectively. The constant parts of the scalar potential M_1 and $M_1+\Delta M_1$ can be interpreted as the constituent masses of the quarks, which are simply the displacements of the current quark masses $\hat{m}$ and m_s due to the potential $S(r)+\Delta S(r)\lambda_s$.

In previous works, for example in the calculation of electromagnetic nucleon form factors [22], we restricted our kinematics to a specific reference frame, that is the Breit frame. This particular choice is sufficient to guarantee local gauge invariance concerning the coupling of the electromagnetic field (for a detailed discussion see Ref. [22]). The Breit frame is specified as follows: the momentum of the initial state is $p=(E,-\vec{q}/2)$, the final momentum is $p'=(E,\vec{q}/2)$ and the 4-momentum of the external field is $q=(0,\vec{q})$ with $p'=p+q$. The constraint of local gauge invariance requires that the bare energies of the nonstrange ($\mathcal{E}_0^q$) and strange ($\mathcal{E}_0^s$) quarks should be equal to each other: $\mathcal{E}_0^q=\mathcal{E}_0^s=\mathcal{E}_0$. In the following we use this requirement for consistency of our calculation. Unitary symmetry breaking at tree level is then contained in the deformation of the bare wave function of the strange quark with respect to the nonstrange one: $u_0^s(\vec{x})\neq u_0^q(\vec{x})$.

The parameters $\{\rho_q,R_q\}$ and $\{\rho_s,R_s\}$ can be fixed from a study of some canonical (electromagnetic and semileptonic) properties of baryons at zeroth order. The parameter ρ_q is related to the nucleon axial charge g_A calculated in zeroth-order (or 3q-core) approximation:

$$g_A=\frac{5}{3}\Big(1-\frac{2\rho_q^2}{1+\frac{3}{2}\rho_q^2}\Big)=\frac{5}{3}\Big(1-\frac{2}{3}[1-\gamma_q]\Big) \tag{20}$$

where

$$\gamma_i=\frac{1-\frac{3}{2}\rho_i^2}{1+\frac{3}{2}\rho_i^2} \tag{21}$$

is the relativistic reduction factor for nonstrange ($i=q$) and strange ($i=s$) quarks (the specific value $\gamma_i=1$ corresponds to the nonrelativistic limit) [2]. Therefore, ρ_q can be replaced by g_A using the matching condition (20). In our calculations we use the value g_A=1.25 [22,23] or $\rho_q=\sqrt{2/13}\simeq 0.392$. The parameter R_q is related to the charge radius of the proton in the zeroth-order approximation as

$$\langle r_E^2\rangle_{LO}^P=\int d^3x\, u_0^{q\,\dagger}(\vec{x})\,\vec{x}^{\,2}\,u_0^q(\vec{x})\;=\;\frac{3R_q^2}{2}\,\frac{1\,+\,\frac{5}{2}\,\rho_q^2}{1\,+\,\frac{3}{2}\,\rho_q^2}. \tag{22}$$

In previous numerical studies R_q is varied in the region from 0.55 fm to 0.65 fm, which corresponds to a change of $\langle r_E^2\rangle_{LO}^P$ from 0.5 to 0.7 fm^2 [22,23]. In the current work we use the central value of $R_q=0.6$ fm.

The values of the parameters ρ_s, R_s can be deduced from the ratios g_A/g_V of the axial (g_A) and vector (g_V) constants in semileptonic decays of hyperons. In zeroth-order approximation following relations for the g_A/g_V ratios are obtained:

$$\begin{aligned}
(g_A/g_V)|_{\Lambda\to pe^-\bar{\nu}_e} &= -r_A && (-0.718\pm 0.015)\,,\\
(g_A/g_V)|_{\Sigma^-\to ne^-\bar{\nu}_e} &= \frac{1}{3}\,r_A && (0.32\pm 0.017)\,,\\
(g_A/g_V)|_{\Xi^-\to\Lambda^0 e^-\bar{\nu}_e} &= -\frac{1}{3}\,r_A && (-0.25\pm 0.05)\,,\\
(g_A/g_V)|_{\Xi^0\to\Sigma^+ e^-\bar{\nu}_e} &= -\frac{5}{3}\,r_A && (-1.32^{+0.21}_{-0.17}\pm 0.05)\,.
\end{aligned}$$

In the brackets (...) we quote the correponding experimental value [29]. The quantity r_A is the ratio of the spatial matrix elements of the axial and vector quark currents:

$$r_A \,=\, \frac{1\,-\,\dfrac{\rho_q^2}{2}\,\kappa_s}{1\,+\,\dfrac{3}{2}\,\rho_q^2\,\kappa_s} = 1\,-\,\frac{2}{3}\,(1-\gamma_{qs})\,, \qquad \kappa_s \,=\, \frac{2\Delta_s}{1\,+\,\Delta_s^2}\,\frac{\rho_s}{\rho_q}\,, \qquad \Delta_s \,=\, \frac{R_s}{R_q} \tag{23}$$

which is related to the relativistic reduction factor γ_s for the $s \to u$ flavor exchange:

$$\gamma_{qs} \,=\, \frac{1\,-\,\dfrac{3}{2}\,\rho_q^2\,\kappa_s}{1\,+\,\dfrac{3}{2}\,\rho_q^2\,\kappa_s} \tag{24}$$

In the $SU(3)$ flavor limit with $R_s = R_q$ and $\rho_s = \rho_q$ (or $\kappa_s = 1$) the factor γ_{qs} reduces to γ_q introduced in Eq. (21) for the $d \to u$ flavor transition. In this study, the parameters ρ_s and R_s are fitted, as will be shown later, by using the baryon mass spectrum as well as to the data for the g_A/g_V ratios. The best choice is: $\rho_s = 0.354$ and $R_s = 0.58$ fm. This results in the value of $r_A = 0.77$, which satisfies the above constraint from semileptonic hyperon decay.

To evaluate the mass shifts of the baryons due to the residual interaction we formulate perturbation theory. In general, the expectation value of an operator $\hat{A}$ is set up as:

$$\langle \hat{A} \rangle = {}^B\langle \phi_0 | \sum_{n=0}^{\infty} \frac{i^n}{n!} \int d^4x_1 \ldots \int d^4x_n T[\mathcal{L}_I(x_1) \ldots \mathcal{L}_I(x_n) \hat{A}] | \phi_0 \rangle_c^B, \tag{25}$$

where the state vector $|\phi_0\rangle$ corresponds to the unperturbed three-quark state ($3q$-core). Superscript "B" in (25) indicates that the matrix elements have to be projected onto the respective baryon states, whereas subscript "c" refers to contributions from connected graphs only. $\mathcal{L}_I(x)$ contained in Eq. (25) is the interaction Lagrangian derived in Eq. (5):

$$\mathcal{L}_I(x) = -\bar{\psi}(x) \Big\{ S(r) i\gamma^5 \frac{\hat{\Phi}(x)}{F} + g_s \gamma^\mu A_\mu^a(x) \frac{\lambda^a}{2} \Big\}\,. \tag{26}$$

For the evaluation of Eq.(25) we apply Wick's theorem with the appropriate propagators for quarks and mesons.

For the quark field we use a Feynman propagator for a fermion in a binding potential with

$$\delta^{mn} i G_\psi^m(x,y) = \langle 0 | T\{ \psi^m(x) \bar{\psi}^n(y) \} | 0 \rangle \tag{27}$$

where m, n are the flavor indices and

$$\begin{aligned} i G_\psi^m(x,y) = {} & \theta(x_0 - y_0) \sum_\alpha \, u_\alpha^m(\vec{x})\, \bar{u}_\alpha^m(\vec{y})\, e^{-i\mathcal{E}_\alpha^m (x_0 - y_0)} \\ & - \theta(y_0 - x_0) \sum_\beta \, v_\beta^m(\vec{x})\, \bar{v}_\beta^m(\vec{y})\, e^{i\mathcal{E}_\beta^m (x_0 - y_0)}\,. \end{aligned} \tag{28}$$

In present study we restrict the expansion of the quark propagator to the ground state with:

$$iG^m_\psi(x,y) \to iG^m_0(x,y) \doteq u^m_0(\vec{x})\,\bar{u}^m_0(\vec{y})\,e^{-i\mathcal{E}^m_0(x_0-y_0)}\,\theta(x_0-y_0). \tag{29}$$

Such a truncation can be considered as an additional regularization of the quark propagator, where in the case of flavor $SU(2)$ intermediate baryon states in loop-diagrams are restricted to N and Δ.

For the meson fields we adopt the free Feynman propagator with

$$i\Delta_{PP'}(x-y) = \langle 0|T\{\Phi_P(x)\Phi_{P'}(y)\}|0\rangle = \delta_{PP'}\int\frac{d^4k}{(2\pi)^4 i}\frac{\exp[-ik(x-y)]}{M_P^2-k^2-i\epsilon}. \tag{30}$$

For the gluon field we use the dressed propagator containing an effective quark-gluon coupling constant $\alpha_s(k^2) = g_s^2(k^2)/(4\pi)$ with a nontrivial momentum dependence. In our consideration we use the Coulomb gauge[1] to separate the contributions of Coulomb (A^a_0) and transverse (A^a_i) gluons in the propagator:

$$i\,\alpha_s\,D^{ab}_{00}(x-y) \;=\; -\,\delta^{ab}\int\frac{d^4k}{(2\pi)^4 i}\frac{e^{-ik(x-y)}}{\vec{k}^{\,2}}\,\alpha_s(k^2) \tag{31}$$

and

$$i\,\alpha_s\,D^{ab}_{ij}(x-y) \;=\; \delta^{ab}\int\frac{d^4k}{(2\pi)^4 i}\frac{e^{-ik(x-y)}}{k^2+i\varepsilon}\Big\{\delta_{ij}-\frac{k_ik_j}{\vec{k}^{\,2}}\Big\}\,\alpha_s(k^2)\,. \tag{32}$$

Following the ideas of the approach to low-energy QCD based on the solutions of the Dyson-Schwinger equations [30] we suppose that the running coupling constant $\alpha_s(k^2)$ includes nontrivial effects of vertex and self-energy corrections, etc. In the present paper, we test a simple analytic form for α_s as suggested in Ref. [30]:

$$\alpha_s(t) \;=\; \frac{\pi}{\omega^6}Dt^2e^{-t/\omega^2} + \frac{2\gamma_m\pi}{\ln\Big[\tau+\Big(1+t/\Lambda^2_{QCD}\Big)^2\Big]}F(t) \tag{33}$$

where $t=-k^2$ is an Euclidean momentum squared, $F(t)=1-\exp(-t/[4m_t^2])$, $\tau=e^2-1$, $\gamma_m=12/(33-2N_f)$, $\Lambda^{N_f=4}_{QCD}=0.234$ GeV, $\omega=0.3$ GeV and $m_t=0.5$ GeV. The functional form of $\alpha_s(t)$ was fitted to the perturbative QCD result in the ultraviolet region (at large momentum squared), and is governed by a single parameter D in the infrared region. In Ref. [30] the parameter $D=(0.884\,\mathrm{GeV})^2$ was adjusted phenomenologically to reproduce properties of pions and kaons described as bound states of constituent quarks. In our considerations we fit the effective coupling with $D=(0.49\,\mathrm{GeV})^2$ such that the $\Delta-N$ mass splitting is reproduced. The running coupling $\alpha_s(t)$ between quarks and gluons should be considered as effective, since it depends on the way its used in phenomenology. Since, in our model, we utilize gluon as well as meson degrees of freedom, it is natural that our fitted value for D is smaller than the one of Ref. [30]. Namely, the relatively small value for D leaves space for meson cloud effects in the infrared region.

---

[1]It can be shown that the results do not depend on the choice of the gauge.

III. BARYON MASS SHIFT WITH IN THE PCQM

In chiral quark models, the mass of the ground-state baryon is given by sum of the contribution of the three-quark core, the finite current quark mass and the mass shift due to the interaction between quarks and meson fields. In the present paper, we also include the gluon induced mass shifts, hence the ground-state baryon mass is written as

$$m_B \;=\; E_{3q} \;+\; \sum_i \gamma_i m_i \;+\; \Delta m_B^M \;+\; \Delta m_B^G \;. \tag{34}$$

The first term E_{3q} is the mass of the three-quark core which is the sum of the bare energies of the ground-state quarks including the subtraction of the spurious center-of-mass (cm) term $E_{\rm cm}$:

$$E_{3q} = 3\mathcal{E}_0 - E_{\rm cm}\,. \tag{35}$$

The second term is the finite current quark mass contribution, the last terms are the meson and gluon cloud induced mass shifts, respectively.

The bare energy of the ground-state quark is the same in magnitude for both the non-strange and strange quarks by construction (see discussion in Section II) and is considered as a free parameter. We also use a unified value of $E_{\rm cm}$ for all baryons. Since $\mathcal{E}_0$ and $E_{\rm cm}$ appear in a linear combination in Eq. (35), we only have one free parameter - the mass of the three-quark core E_{3q}. We fix E_{3q} from a fit of the nucleon mass by including all one-loop effects: $E_{3q} = 1612.4$ MeV. The shift of the quark energy due to the finite current quark mass $m_i = \hat{m}$, m_s is calculated perturbatively and is given by a term linear in m_i (see details in Refs. [22,23]):

$$\mathcal{E}_0 \;\to\; \mathcal{E}_0(m_i) \;=\; \mathcal{E}_0 \;+\; \gamma_i\, m_i + o(m_i)\,. \tag{36}$$

where m_i and γ_i are the values for the current quark mass ($\hat{m}$ or m_s) and for the relativistic reduction factor (γ_q or γ_s). From the exact solution of the Dirac equation including the current quark mass term it can be shown that higher order corrections $o(m_i)$ are negligible. In the case of the nonstrange quark the linear term $\gamma_q\hat{m}$ gives a correction of the order of 1%, whereas the term with $o(\hat{m})$ is about 10^{-2}% of $\mathcal{E}_0$. For the strange quark the linear term is more important yielding a correction of ~ 20%, the higher-order term $o(m_s)$ is suppressed giving a contribution of only 2% of $\mathcal{E}_0$.

In the PCQM, the mass shift $\Delta m_B = \Delta m_B^M \;+\; \Delta m_B^G$ is evaluated perturbatively. In the one-loop approximation it is given by

$$\Delta m_B = {}^B\langle\phi_0| \sum_{n=1}^{2} \frac{i^n}{n!} \int i\delta(t_1) d^4x_1 \cdots d^4x_n T[\mathcal{L}_I(x_1)\cdots\mathcal{L}_I(x_n)]|\phi_0\rangle_c^B \tag{37}$$

where $\mathcal{L}_I$ is the interaction Lagrangian of quarks with meson and gluon fields. The diagrams contributing to Δm_B are shown in Fig.1 (meson contribution) and in Fig.2 (gluon contribution).

The meson induced baryon mass shift Δm_B^M consists of the contribution of the meson cloud (Fig.1a) and the meson exchange (Fig.1b) diagram. The expression for the meson contribution to the baryon mass shift is given by

$$\Delta m_B^M \,=\, \sum_{\Phi=\pi,K,\eta} \Delta m_B^\Phi \,=\, \sum_{\Phi=\pi,K,\eta} \,[\,\Delta m_B^{\Phi[\rm C]}(M_\Phi^2) \,+\, \Delta m_B^{\Phi[\rm E]}(M_\Phi^2)\,] \tag{38}$$

where $\Delta m_B^{\Phi[\rm C]}$ is the contribution of the diagram of Fig.1a and $\Delta m_B^{\Phi[\rm E]}$ is related to the diagram of Fig.1b. The partial contribution of the π, K, and η-meson cloud to the baryon mass shifts are written as

$$\Delta m_B^{\pi[\rm C]}(M_\pi^2) = d_B^{\pi[\rm C]}\,\Pi_{[qq,qq]}(M_\pi^2) \tag{39}$$

$$\Delta m_B^{K[\rm C]}(M_K^2) = d_B^{K[\rm C1]}\,\Pi_{[qs,sq]}(M_K^2) \,+\, d_{B[sq,qs]}^{K[\rm C2]}\,\Pi_{[sq,qs]}(M_K^2) \tag{40}$$

$$\Delta m_B^{\eta[\rm C]}(M_\eta^2) = d_B^{\eta[\rm C1]}\,\Pi_{[qq,qq]}(M_\eta^2) \,+\, d_B^{\eta[\rm C2]}\,\Pi_{[ss,ss]}(M_\eta^2) \tag{41}$$

$$\Delta m_B^{\pi[\rm E]}(M_\pi^2) = d_B^{\pi[\rm E]}\,\Pi_{[qq,qq]}(M_\pi^2) \tag{42}$$

$$\Delta m_B^{K[\rm E]}(M_K^2) = d_B^{K[\rm E1]}\,\Pi_{[qs,sq]}(M_K^2) \,+\, d_B^{K[\rm E2]}\,\Pi_{[sq,qs]}(M_K^2) \tag{43}$$

$$\Delta m_B^{\eta[\rm E]}(M_\eta^2) = d_B^{\eta[\rm E1]}\,\Pi_{[qq,qq]}(M_\eta^2) \,+\, d_B^{\eta[\rm E2]}\,\Pi_{[qq,ss]}(M_\eta^2) \,+\, d_B^{\eta[\rm E3]}\,\Pi_{[ss,ss]}(M_\eta^2). \tag{44}$$

Here, $d_B^{\Phi[\rm J]}$ are recoupling coefficients which are listed in Table I and $\Pi_{[ij,kl]}(M_\Phi^2)$ are the meson-loop integrals

$$\Pi_{[ij,kl]}(M_\Phi^2) \,=\, -\Big(\frac{g_A}{\pi F}\Big)^2 \int\limits_0^\infty dp\, p^4\, \frac{G_{ij}(p^2)\, G_{kl}(p^2)}{p^2 \,+\, M_\Phi^2}\,. \tag{45}$$

The quark-meson transition form factor $G_{ij}(p^2)$ is given by

$$G_{ij}(p^2) \,=\, \rho_{ij}\,\Big(\frac{\Delta_{ij}}{\Delta_i\,\Delta_j}\Big)^{5/2}\,\Big(\frac{\rho_i\Delta_j + \rho_j\Delta_i}{2\rho_q}\Big)\,\Big(1 + \frac{5\rho_q^2}{2-\rho_q^2}\,[\Delta_{ij} \,-\, 1]\Big)\,F_{ij}(p^2) \tag{46}$$

where

$$\Delta_{ij} = \frac{2\,\Delta_i^2\,\Delta_j^2}{\Delta_i^2 \,+\, \Delta_j^2}\,, \qquad\qquad \rho_{ij} = \frac{2+3\rho_q^2}{(2+3\rho_i^2)^{1/2}(2+3\rho_j^2)^{1/2}} \tag{47}$$

and $F_{ij}(p^2)$ is the meson-quark transition form factor normalized to unity at $p^2 = 0$:

$$F_{ij}(p^2) = \exp\Big(-\frac{p^2\,R^2}{4}\,\Delta_{ij}\Big)\,\Big[1 \,-\, \frac{p^2\,R^2}{2}\,\frac{\rho_q^2\,\Delta_{ij}^2}{2 \,-\, 6\rho_q^2 \,+\, 5\,\rho_q^2\,\Delta_{ij}}\Big]\,. \tag{48}$$

The gluon induced baryon mass shift Δm_B^G consists of the contribution of the gluon cloud (Fig.2a) and the exchange (Fig.2b) diagram. As in the previous case we separate the gluon induced mass shifts Δm_B^G into terms arising from the gluon cloud ($\Delta m_B^{\rm E[C]}$ and $\Delta m_B^{\rm M[C]}$) and the gluon exchange ($\Delta m_B^{\rm E[E]}$ and $\Delta m_B^{\rm M[E]}$) corrections. A corresponding index is introduced

in square brackets. In addition, the index E or M indicates contributions of Coulomb or transverse gluons, respectively:

$$\Delta m_B^G \,=\, \Delta m_B^{\rm G[C]} \,+\, \Delta m_B^{\rm G[E]}\,, \tag{49}$$

$$\Delta m_B^{\rm G[C]} \,=\, \Delta m_B^{\rm E[C]} \,+\, \Delta m_B^{\rm M[C]}\,, \qquad \Delta m_B^{\rm G[E]} \,=\, \Delta m_B^{\rm E[E]} \,+\, \Delta m_B^{\rm M[E]}\,, \tag{50}$$

where

$$\Delta m_B^{\rm I[C]} = d_B^{\rm I[C1]}\,\Sigma_{qq}^{\rm I} \,+\, d_B^{\rm I[C2]}\,\Sigma_{ss}^{\rm I}\,,$$

$$\Delta m_B^{\rm I[E]} = d_B^{\rm I[E1]}\,\Sigma_{qq}^{\rm I} \,+\, d_B^{\rm I[E2]}\,\Sigma_{qs}^{\rm I} \,+\, d_B^{\rm I[E3]}\,\Sigma_{ss}^{\rm I}\,.$$

with ${\rm I} = {\rm E}, {\rm M}$. Here, $d_B^{\rm I[J]}$ are the recoupling coefficients which are listed in Table II and $\Sigma_{q_1q_2}^{\rm E(M)}$ are the gluon-loop integrals with

$$\Sigma_{q_1q_2}^{\rm E} = \frac{1}{\pi}\int\limits_0^\infty dp\,\alpha_s(p^2)\,G_{\rm E}^{q_1}(p^2)\,G_{\rm E}^{q_2}(p^2) \tag{51}$$

$$\Sigma_{q_1q_2}^{\rm M} = \frac{1}{\pi}\int\limits_0^\infty dp\,\alpha_s(p^2)\,G_{\rm M}^{q_1}(p^2)\,G_{\rm M}^{q_2}(p^2).$$

The charge and magnetic form factors $G_{\rm E}^i$ and $G_{\rm M}^i$ with $i = q, s$ of the constituent quarks are calculated at leading order (LO) or at tree level (without inclusion of the dressing by meson and gluon cloud corrections) using the solutions of the Dirac equation for nonstrange (18) and strange (19) quarks:

$$G_{\rm E}^i(p^2) = \int\limits_0^\infty dx\,x^2\,j_0(px)\Big\{\,[g_0^i(x)]^2 + [f_0^i(x)]^2\,\Big\} \,=\, \Big(1 - \frac{\rho_i^2}{1+\frac{3}{2}\rho_i^2}\frac{p^2R_i^2}{4}\Big)\,\exp\Big(-\frac{p^2R_i^2}{4}\Big)\,, \tag{52}$$

$$G_{\rm M}^i(p^2) = \int\limits_0^\infty dx\,x^2\,j_1(px)\,\Big\{\,2\,g_0^i(x)\,f_0^i(x)\,\Big\} \,=\, 2p\,\frac{\rho_i\,R_i}{1+\frac{3}{2}\rho_i^2}\,\exp\Big(-\frac{p^2R_i^2}{4}\Big)\,,$$

where g_0^i and f_0^i are the upper and lower components of the Dirac spinors; j_0 and j_1 are the spherical Bessel functions. In Fig.3 we indicate the momentum dependence of the effective coupling as function of three-momentum squared (solid line). For comparison we also show the functions $\alpha_s(p^2)$ used in Ref. [30] (long-dashed line) and the one referring to perturbative one-loop QCD (dotted line). The infrared part of $\alpha_s(p^2)$ in the present calculation is much smaller than the one used in Ref. [30]. This again can be explained by the fact that in the infrared domain both gluon and meson degrees of freedom are strongly interacting with the quark fields. It leads in turn to a relative suppression of the effective running constant $\alpha_s(p^2)$ at low p^2 with respect to the original fit. The residual gluon contribution is therefore smaller than in the approach [30] where mesonic degrees of freedom are not taken into account in the description of baryon structure.

It is convenient to separate the value of the baryon mass m_B into a term related to the chiral limit $\overset{0}{m}_B$ (defined in the limit $\hat{m}, m_s \to 0$ with $\rho_s = \rho_q$ and $R_s = R_q$) and a term referring to the violation of chiral and unitary flavor symmetry δm_B:

$$m_B \, = \overset{0}{m}_B \, + \delta m_B \, . \tag{53}$$

Here

$$\begin{aligned} \overset{0}{m}_B \; &= E_{3q} \, + \, \Delta \, \overset{0\,M}{m}_B \, + \Delta \, \overset{0\,G}{m}_B \\ \Delta \, \overset{0\,M}{m}_B \; &= \sum_{\Phi=\pi,K,\eta} \left\{ \, \Delta m_B^{\Phi[\mathrm{C}]}(0) \, + \, \Delta m_B^{\Phi[\mathrm{E}]}(0) \, \right\} \Big|_{\rho_s=\rho_q \, , \, R_s=R_q} \, , \\ \Delta \, \overset{0\,G}{m}_B \; &= \left\{ \, \Delta m_B^{\mathrm{G[C]}} \, + \, \Delta m_B^{\mathrm{G[E]}} \, \right\} \Big|_{\rho_s=\rho_q \, , \, R_s=R_q} \, . \end{aligned} \tag{54}$$

Meson loops also contribute to $\overset{0}{m}_B$, since in the chiral limit quarks also interact with massless mesons. The separate contributions of the three-quark core (E_{3q}), meson ($\Delta \, \overset{0\,M}{m}_B$) and gluon ($\Delta \, \overset{0\,G}{m}_B$) cloud terms are:

$$E_{3q} = 1612.4 \text{ MeV} \tag{55}$$

for both flavor octet and decuplet baryons. For the octet baryons we get

$$\begin{aligned} \Delta \, \overset{0\,M}{m}_{B^8} \; &= -254.6 \text{ MeV} - 148.6 \text{ MeV} = -403.2 \text{ MeV} \\ \Delta \, \overset{0\,G}{m}_{B^8} \; &= 565.2 \text{ MeV} - 946.0 \text{ MeV} = -380.8 \text{ MeV} \end{aligned} \tag{56}$$

while for the decuplet we have

$$\begin{aligned} \Delta \, \overset{0\,M}{m}_{B^{10}} \; &= -254.6 \text{ MeV} - 42.5 \text{ MeV} = -297.1 \text{ MeV} \\ \Delta \, \overset{0\,G}{m}_{B^{10}} \; &= 565.2 \text{ MeV} - 755.6 \text{ MeV} = -190.4 \text{ MeV}. \end{aligned} \tag{57}$$

In Eqs. (56) and (57) we indicate the contributions of the cloud (Figs.1a and 2a) and exchange (Figs.1b and 2b) diagrams derived in Eq. (54). Only the exchange diagrams of Figs.1b and 2b contribute to the octet-decuplet mass splitting in the chiral limit:

$$\delta = \overset{0}{m}_{B^{10}} - \overset{0}{m}_{B^8} = \delta^M + \delta^G \tag{58}$$

where $\delta^M = 106.1$ MeV and $\delta^G = 190.4$ MeV are the partial meson and gluon contributions.

The octet baryon mass ($\overset{0}{m}_{B^8}$) and a finite decuplet-octet baryon mass difference, both defined in the chiral limit, are the natural ingredients (or input parameters) of chiral effective Lagrangians (see, e.g. Refs. [27,31–37]). Our numerical values for these quantities are:

$$\begin{aligned} \overset{0}{m}_{B^8} \; &= 828.5 \text{ MeV} \, , \qquad B^8 = N, \Lambda, \Sigma, \Xi \\ \overset{0}{m}_{B^{10}} \; &= 1124.9 \text{ MeV} \, , \qquad B^{10} = \Delta, \Sigma^*, \Xi^*, \Omega \\ \delta \; &= 296.4 \text{ MeV} \approx 300 \text{ MeV} \, . \end{aligned} \tag{59}$$

Our value for δ is close to the experimental result for the $\Delta - N$ mass splitting. Inclusion of symmetry breaking corrections does not affect the value for $\overset{0}{m}_\Delta - \overset{0}{m}_N$ evaluated in the chiral limit. For comparison we quote the parameters of the average octet baryon mass

$\overset{0}{m}_{B^8}$ and the mass difference δ as predicted or adjusted in other effective chiral approaches. The value of $\overset{0}{m}_{B^8}$ was estimated in heavy baryon chiral perturbation theory [32] with $\overset{0}{m}_{B^8}=770\pm110$ MeV. In chiral perturbation theory with infrared regularization [35] $\overset{0}{m}_{B^8}$ decreases from 733 MeV at third order of the chiral expansion to 653 MeV at fourth order. In Ref. [33] the input parameter $\delta = 300$ MeV, which is very close to ours, was used in the description of baryon magnetic moments. A detailed analysis of baryon (nucleon) masses using a chiral extrapolation of lattice data was done in Refs. [36,37]. In Ref. [36] the meson-loop contribution to the $\Delta - N$ mass splitting for different values of M_π^2 (including the chiral limit $M_\pi^2 = 0$ and the physical point) was studied in both schemes (quenched and full) of lattice QCD. The pion cloud contributes not more than one third to the observed $\Delta - N$ mass splitting. For a specific choice of the regulator parameter meson loops result in about 50 MeV in the full scheme of lattice QCD. The remaining contribution to the splitting is probably attributed to short-range effects, like gluon exchange. Below we show that the lattice finding corresponds to the situation derived in our model: the partial contributions of meson and gluon cloud to δ are 1/3 and 2/3, respectively. In Ref. [37] a value of $\overset{0}{m}_N\simeq 880$ MeV was deduced with baryon chiral perturbation theory up to order p^4.

In Table III we give the results for the partial and total mass shifts of the octet and decuplet baryons for our set of parameters: $\rho_q = \sqrt{2/13}$, $\rho_s = 0.354$, $R_q = 0.6$ fm and $R_s = 0.58$ fm. Table IV contains the results for the case when the parameters of nonstrange and strange quarks are degenerate with $\rho_q = \rho_s = \sqrt{2/13}$ and $R_q = R_s = 0.6$ fm. The meson cloud provides a significant downward shift, e.g., for nucleon it is about -300 MeV. Thereby the dominant contribution is due to pion loops with ~ -260 MeV. The two sets of results, with and without inclusion of flavor symmetry breaking, presented in Tables III and IV display no big difference. The results differ slightly in particular for hyperons due to the modification of the kaon cloud. Meson loop effects also provide considerable mass splittings. For example, they contribute 110 MeV to the splitting $m_\Xi - m_N$, which is of considerable size. However, the meson induced mass shifts are not sufficient to explain the full observed mass splittings. For example, meson effect yield only 100 MeV to the mass difference $m_\Delta - m_N$, and also only 40 MeV to $m_\Sigma - m_\Lambda$. The observed splittings are about 300 MeV and 75 MeV, respectively. An additional mechanism, like effective gluon exchange, is needed to explain the observed splittings. The important ingredients to partially reproduce the mass shifts are at this level already taken into account: breaking of unitary flavor symmetry, meson cloud effects and finite current quark masses (especially for the strange quark).

In a next step we also include the quantum corrections of the gluon cloud to the baryon masses. The numerical results for the mass shifts induced by the gluon corrections are given in Tables V and VI. Again, we present our predictions for the two sets of parameters $\rho_q = \sqrt{2/13}$, $\rho_s = 0.354$, $R_q = 0.6$ fm and $R_s = 0.58$ fm (Table V) and $\rho_q = \rho_s = \sqrt{2/13}$ and $R_q = R_s = 0.6$ fm (Table VI). In the "symmetric" case, where the bare parameters of the quark wave functions are identical, gluon cloud corrections to the baryon octet and decuplet mass shifts are degenerate.

Combining all effects we can reasonably reproduce all the observed mass differences. In Table VII we give the full results for the ground-state baryon masses indicating all mechanisms (bare mass, mass shifts induced by the current quark mass, meson and gluon cloud) for the best choice of free parameters. For the experimental data we quote the masses of

$m_P, m_{\Lambda^0}, m_{\Sigma^+}, m_{\Xi^-}, m_{\Delta^+}, m_{\Sigma^{*+}}, m_{\Xi^{*-}}$ and m_{Ω^-}. For completeness, in Table VIII we also list our results for the symmetric set of free parameters. Obviously, in the latter case the description of the hyperon mass spectrum deteriorates with respect to the "asymmetric case" where the mechanism of $SU(3)$ flavor symmetry breaking is included. In the following we only discuss the full results presented in Table VII. The predicted mass of the Σ baryon is heavier than that of the Λ hyperon consistent with the experimental observation, although the obtained difference is a little smaller than the data. The difference is generated both by meson and gluon induced mass shifts, but the mesonic effect is about 40 MeV and hence more important than the one due to the gluon. A slightly more "asymmetric parameter" set results in a larger gluon induced mass difference and hence a better fit to the $\Sigma - \Lambda$ mass splitting, but the overall mass prediction gets worse. Next we illustrate the validity of our model in the context of the Gell-Mann-Okubo mass relations (4). Both the meson and gluon induced mass shifts well satisfy the relations separately, based on our construction of $SU(6)$ baryon wave functions; hence the predictions for the total masses also satisfy these relations. Moreover, our model generates small violations of the relations which are qualitatively consistent with data, i.e. L.H.S. > R.H.S. in the octet and L.H.S. > Center > R.H.S. in the decuplet. These phenomenologically consistent violations are provided by the meson cloud, while the gluon corrections give opposite signs. Finally, we comment on the $SU(3)$ breaking effects on the meson-nucleon sigma terms, which are fully discussed in Ref. [25]. We list the results in Table IX, where the additional effect is found to be negligibly small. For example, the obtained πN sigma term of 54.6 MeV is merely 0.1 MeV smaller than in the case of the symmetric parameter set. This is naturally to be expected since the nucleon does not contain strange valence quarks and hence only kaon loop diagrams are affected by the flavor symmetry breaking. Again, the "asymmetric parameter" set is more important when considering hyperons. Therefore, the results for the meson-nucleon sigma terms indicated in a recent paper [25], where the "symmetric parameter" set is employed, are essentially reasonable.

IV. SUMMARY

We have studied the mass spectrum of the ground-state baryons in the perturbative chiral quark model. We have extended the model by including quantum corrections of the gluon and by setting up a more realistic mechanism for $SU(3)$ flavor symmetry violation. Both, meson and gluon induced mass shifts are important ingredients to quantitatively reproduce the absolute baryon mass spectrum and the resulting mass splittings. The mass splitting between the octet and the decuplet baryons is dominantly generated by the gluon mechanism. In particular, the $\Delta - N$ mass difference is saturated by 1/3 by the meson cloud, while gluon corrections contribute about 2/3. This finding is consistent with a recent lattice simulation [36], where a sizable nucleon-Δ mass splitting is even observed in the quenched approximation. For the mass scales within each multiplet the meson mechanism is found to be the most important effect, as demonstrated for example for the $\Sigma - \Lambda$ mass difference. In addition, the meson mechanism is qualitatively consistent with the small violations of the

Gell-Mann-Okubo mass relations.

Acknowledgments
This work was supported by the Deutsche Forschungsgemeinschaft (DFG) under contracts FA67/25-3 and GRK683.

REFERENCES

[1] F. E. Close, *An Introduction To Quarks And Partons*, (Academic Press, New York, 1979).

[2] J. F. Donoghue, E. Golowich and B. R. Holstein, *Dynamics Of The Standard Model*, Cambridge Monogr. Part. Phys. Nucl. Phys. Cosmol. **2**, 1 (1992).

[3] A. De Rujula, H. Georgi and S. L. Glashow, Phys. Rev. D **12**, 147 (1975).

[4] N. Isgur and G. Karl, Phys. Rev. D **18**, 4187 (1978).

[5] L. Y. Glozman and D. O. Riska, Phys. Rept. **268**, 263 (1996) [arXiv:hep-ph/9505422].

[6] L. Y. Glozman, W. Plessas, K. Varga and R. F. Wagenbrunn, Phys. Rev. D **58**, 094030 (1998) [arXiv:hep-ph/9706507].

[7] L. Y. Glozman, Z. Papp, W. Plessas, K. Varga and R. F. Wagenbrunn, Phys. Rev. C **57**, 3406 (1998) [arXiv:nucl-th/9705011].

[8] L. Y. Glozman, Z. Papp, W. Plessas, K. Varga and R. F. Wagenbrunn, Phys. Rev. C **61**, 019804 (2000).

[9] A. Valcarce, F. Fernandez, P. Gonzalez and V. Vento, Phys. Lett. B **367**, 35 (1996) [arXiv:nucl-th/9509009].

[10] F. Fernandez, A. Valcarce and P. Gonzalez, Few Body Syst. Suppl. **10** (1999) 395.

[11] H. Garcilazo, A. Valcarce and F. Fernandez, Phys. Rev. C **63**, 035207 (2001).

[12] H. Garcilazo and A. Valcarce, Phys. Rev. C **68**, 035207 (2003) [arXiv:hep-ph/0308023].

[13] M. Furuichi and K. Shimizu, Phys. Rev. C **65**, 025201 (2002).

[14] N. Kaiser, P. B. Siegel and W. Weise, Phys. Lett. B **362**, 23 (1995) [arXiv:nucl-th/9507036].

[15] J. C. Nacher, A. Parreno, E. Oset, A. Ramos, A. Hosaka and M. Oka, Nucl. Phys. A **678**, 187 (2000) [arXiv:nucl-th/9906018].

[16] J. Nieves and E. Ruiz Arriola, Phys. Rev. D **64**, 116008 (2001) [arXiv:hep-ph/0104307].

[17] T. Inoue, E. Oset and M. J. Vicente Vacas, Phys. Rev. C **65**, 035204 (2002) [arXiv:hep-ph/0110333].

[18] S. Capstick, Phys. Rev. D **46**, 1965 (1992).

[19] F. Cardarelli, E. Pace, G. Salme and S. Simula, Phys. Lett. B **397**, 13 (1997) [arXiv:nucl-th/9609047].

[20] O. Krehl, C. Hanhart, S. Krewald and J. Speth, Phys. Rev. C **62**, 025207 (2000) [arXiv:nucl-th/9911080].

[21] E. Hernandez, E. Oset and M. J. Vicente Vacas, Phys. Rev. C **66**, 065201 (2002) [arXiv:nucl-th/0209009].

[22] V. E. Lyubovitskij, T. Gutsche and A. Faessler, Phys. Rev. C **64**, 065203 (2001) [arXiv:hep-ph/0105043].

[23] V. E. Lyubovitskij, T. Gutsche, A. Faessler and E. G. Drukarev, Phys. Rev. D **63**, 054026 (2001) [arXiv:hep-ph/0009341].

[24] V. E. Lyubovitskij, T. Gutsche, A. Faessler and R. Vinh Mau, Phys. Lett. B **520**, 204 (2001) [arXiv:hep-ph/0108134]; Phys. Rev. C **65**, 025202 (2002) [arXiv:hep-ph/0109213]; V. E. Lyubovitskij, P. Wang, T. Gutsche and A. Faessler, Phys. Rev. C **66**, 055204 (2002) [arXiv:hep-ph/0207225]; F. Simkovic, V. E. Lyubovitskij, T. Gutsche, A. Faessler and S. Kovalenko, Phys. Lett. B **544**, 121 (2002) [arXiv:hep-ph/0112277]; K. Pumsa-ard, V. E. Lyubovitskij, T. Gutsche, A. Faessler and S. Cheedket, Phys. Rev. C **68**, 015205 (2003) [arXiv:hep-ph/0304033].

[25] T. Inoue, V. E. Lyubovitskij, T. Gutsche and A. Faessler, Phys. Rev. C **69**, 035207 (2004) [arXiv:hep-ph/0311275].
[26] H. Leutwyler, Nucl. Phys. B **179**, 129 (1981); D. Diakonov and V. Y. Petrov, Nucl. Phys. B **245**, 259 (1984); G. V. Efimov and M. A. Ivanov, *The Quark Confinement Model of Hadrons*, (IOP Publishing, Bristol & Philadelphia, 1993).
[27] J. Gasser, M. E. Sainio and A. Svarc, Nucl. Phys. B **307**, 779 (1988).
[28] J. Gasser and H. Leutwyler, Phys. Rept. **87**, 77 (1982).
[29] K. Hagiwara *et al.* [Particle Data Group Collaboration], Phys. Rev. D **66**, 010001 (2002).
[30] P. Maris and P. C. Tandy, Phys. Rev. C **60**, 055214 (1999) [arXiv:nucl-th/9905056]; C. D. Roberts and S. M. Schmidt, Prog. Part. Nucl. Phys. **45**, S1 (2000) [arXiv:nucl-th/0005064].
[31] E. Jenkins, M. E. Luke, A. V. Manohar and M. J. Savage, Phys. Lett. B **302**, 482 (1993) [Erratum-ibid. B **388**, 866 (1996)] [arXiv:hep-ph/9212226]; M. N. Butler, M. J. Savage and R. P. Springer, Nucl. Phys. B **399**, 69 (1993) [arXiv:hep-ph/9211247].
[32] B. Borasoy and U. G. Meissner, Annals Phys. **254**, 192 (1997) [arXiv:hep-ph/9607432].
[33] L. Durand and P. Ha, Phys. Rev. D **58**, 013010 (1998) [arXiv:hep-ph/9712492].
[34] T. Becher and H. Leutwyler, Eur. Phys. J. C **9**, 643 (1999) [arXiv:hep-ph/9901384].
[35] P. J. Ellis and K. Torikoshi, Phys. Rev. C **61**, 015205 (2000) [arXiv:nucl-th/9904017].
[36] R. D. Young, D. B. Leinweber, A. W. Thomas and S. V. Wright, Phys. Rev. D **66**, 094507 (2002) [arXiv:hep-lat/0205017].
[37] M. Procura, T. R. Hemmert and W. Weise, Phys. Rev. D **69**, 034505 (2004) [arXiv:hep-lat/0309020].

TABLES

TABLE I. Meson recoupling coefficients for the octet and decuplet baryons in units of 1/400.

$d_B^{\Phi[J]}$	π[C]	K[C1]	K[C2]	η[C1]	η[C2]	π[E]	K[E]	η[E1]	η[E2]	η[E3]
N	81	54	0	9	0	90	0	- 6	0	0
Λ	54	36	36	6	12	54	36	- 6	0	0
Σ	54	36	36	6	12	6	60	2	16	0
Ξ	27	18	72	3	24	0	60	0	16	8
Δ	81	54	0	9	0	18	0	6	0	0
Σ^*	54	36	36	6	12	6	24	2	-8	0
Ξ^*	27	18	72	3	24	0	24	0	-8	8
Ω	0	0	108	0	36	0	0	0	0	24

TABLE II. Gluon recoupling coefficients for the octet and decuplet baryons in units of 1/9.

$d_B^{I[J]}$	E[C1]	E[C2]	M[C1]	M[C2]	E[E1]	E[E2]	E[E3]	M[E1]	M[E2]	M[E3]
N	36	0	-72	0	-36	0	0	-24	0	0
Λ	24	12	-48	-24	-12	-24	0	-24	0	0
Σ	24	12	-48	-24	-12	-24	0	8	-32	0
Ξ	12	24	-24	-48	0	-24	-12	0	-32	8
Δ	36	0	-72	0	-36	0	0	24	0	0
Σ^*	24	12	-48	-24	-12	-24	0	8	16	0
Ξ^*	12	24	-24	-48	0	-24	-12	0	16	8
Ω	0	36	0	-72	0	0	-36	0	0	24

TABLE III. Baryon mass shifts (in units of MeV) induced by the meson cloud for the parameter set $\rho_q = \sqrt{2/13}$, $\rho_s = 0.354$, $R_q = 0.6$ fm and $R_s = 0.58$ fm.

$\Delta m_B^{\Phi[\mathrm{J}]}$	π[C]	K[C]	η[C]	π[E]	K[E]	η[E]	Total
N	−125.2	−40.0	−6.2	−139.1	0	4.1	−306.5
Λ	−83.5	−53.4	−11.5	−83.5	−26.7	4.1	−254.5
Σ	−83.5	−53.4	−11.5	−9.3	−44.5	−11.8	−214.0
Ξ	−41.7	−66.7	−16.9	0	−44.5	−15.3	−185.1
Δ	−125.2	−40.0	−6.2	−27.8	0	−4.1	−203.3
Σ^*	−83.5	−53.4	−11.5	−9.3	−17.8	3.8	−171.7
Ξ^*	−41.7	−66.7	−16.9	0	−17.8	0.3	−142.8
Ω	0	−80.1	−22.2	0	0	−14.8	−117.1

TABLE IV. Baryon mass shifts (in units of MeV) induced by the meson cloud for the parameter set $\rho_q = \rho_s = \sqrt{2/13}$ and $R_q = R_s = 0.6$ fm.

$\Delta m_B^{\Phi[\mathrm{J}]}$	π[C]	K[C]	η[C]	π[E]	K[E]	η[E]	Total
N	−125.2	−42.3	−6.2	−139.1	0	4.1	−308.7
Λ	−83.5	−56.4	−12.3	−83.5	−28.2	4.1	−259.8
Σ	−83.5	−56.4	−12.3	−9.3	−47.0	−12.3	−220.8
Ξ	−41.7	−70.6	−18.5	0	−47.0	−16.4	−194.2
Δ	−125.2	−42.3	−6.2	−27.8	0	−4.1	−205.6
Σ^*	−83.5	−56.4	−12.3	−9.3	−18.8	4.1	−176.2
Ξ^*	−41.7	−70.6	−18.5	0	−18.8	0	−149.6
Ω	0	−84.7	−24.7	0	0	−16.4	−125.8

TABLE V. Baryon mass shifts (in units of MeV) induced by the gluon cloud for the parameter set $\rho_q = \sqrt{2/13}$, $\rho_s = 0.354$, $R_q = 0.6$ fm and $R_s = 0.58$ fm.

$\Delta m_B^{\mathrm{I[J]}}$	E[C]	M[C]	E[E]	M[E]	Total
N	850.8	−285.6	−850.8	−95.2	−380.8
Λ	870.9	−274.2	−870.4	−95.2	−368.9
Σ	870.9	−274.2	−870.4	−87.3	−361.0
Ξ	890.9	−262.7	−890.4	−91.1	−353.3
Δ	850.8	−285.7	−850.8	95.2	−190.4
Σ^*	870.9	−274.2	−870.4	91.2	−182.4
Ξ^*	890.9	−262.7	−890.4	87.4	−174.8
Ω	910.9	−251.2	−910.9	83.7	−167.5

TABLE VI. Baryon mass shifts (in units of MeV) induced by the gluon cloud for the parameter set $\rho_q = \rho_s = \sqrt{2/13}$ and $R_q = R_s = 0.6$ fm.

$\Delta m_B^{\mathrm{I[J]}}$	E[C]	M[C]	E[E]	M[E]	Total
N, Λ, Σ, Ξ	850.8	−285.6	−850.8	−95.2	−380.8
$\Delta, \Sigma^*, \Xi^*, \Omega$	850.8	−285.6	−850.8	95.2	−190.4

TABLE VII. Full model results for the baryon mass spectrum (in units of MeV) for the set of parameters $\rho_q = \sqrt{2/13}$, $\rho_s = 0.354$, $R_q = 0.6$ fm and $R_s = 0.58$ fm.

	Core	Quark	Mesons	Gluons	Total	Data
m_N	1612.4	13.1	−306.4	−380.8	938.3	938.3
m_Λ	1612.4	128.3	−254.4	−368.9	1117.4	1115.7
m_Σ	1612.4	128.3	−213.9	−361.0	1165.9	1189.4
m_Ξ	1612.4	243.5	−185.1	−353.3	1317.5	1321.3
m_Δ	1612.4	13.1	−203.4	−190.4	1231.8	1231.6
m_{Σ^*}	1612.4	128.3	−171.6	−182.4	1386.7	1382.8
m_{Ξ^*}	1612.4	243.5	−142.9	−174.8	1538.3	1535.0
m_Ω	1612.4	358.6	−117.1	−167.5	1686.5	1672.5

TABLE VIII. Full model results for the baryon mass spectrum (in units of MeV) for the set of parameters $\rho_q = \rho_s = \sqrt{2/13}$ and $R_q = R_s = 0.6$ fm.

	Core	Quark	Mesons	Gluons	Total	Data
m_N	1612.4	13.1	−308.8	−380.8	935.9	938.3
m_Λ	1612.4	118.1	−259.8	−380.8	1089.9	1115.7
m_Σ	1612.4	118.1	−220.9	−380.8	1128.8	1189.4
m_Ξ	1612.4	223.1	−194.3	−380.8	1260.4	1321.3
m_Δ	1612.4	13.1	−205.7	−190.4	1229.4	1231.6
m_{Σ^*}	1612.4	118.1	−176.2	−190.4	1363.9	1382.8
m_{Ξ^*}	1612.4	223.1	−149.6	−190.4	1495.5	1535.0
m_Ω	1612.4	328.2	−125.8	−190.4	1624.4	1672.5

TABLE IX. Meson-nucleon sigma terms (in units of MeV) for the set of parameter (I) $\rho_q = \sqrt{2/13}$, $\rho_s = 0.354$, $R_q = 0.6$ fm and $R_s = 0.58$ fm, and (II) $\rho_q = \rho_s = \sqrt{2/13}$ and $R_q = R_s = 0.6$ fm

Set	$\sigma_{\pi N}$	σ^u_{KN}	σ^d_{KN}	$\sigma_{\eta N}$
I	54.6	417.1	351.7	93.0
II	54.7	419.2	353.4	96.3

FIGURES

Fig.1: Meson loop diagrams contributing to the baryon energy shift:
meson cloud (1a) and meson exchange diagram (1b).

Fig.2: Gluon loop diagrams contributing to the baryon energy shift:
gluon cloud (2a) and gluon exchange diagram (2b).

Fig.3: Effective running couplings $\alpha_s(p^2)$: i) used in the present study (solid line), ii) used in ref. [30] with the original parameterization (long-dashed line) and iii) used in perturbative QCD (dotted line).

(a) (b)

Fig.1

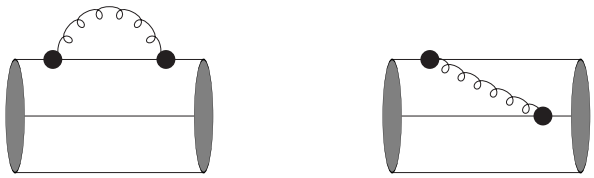

(a) (b)

Fig.2

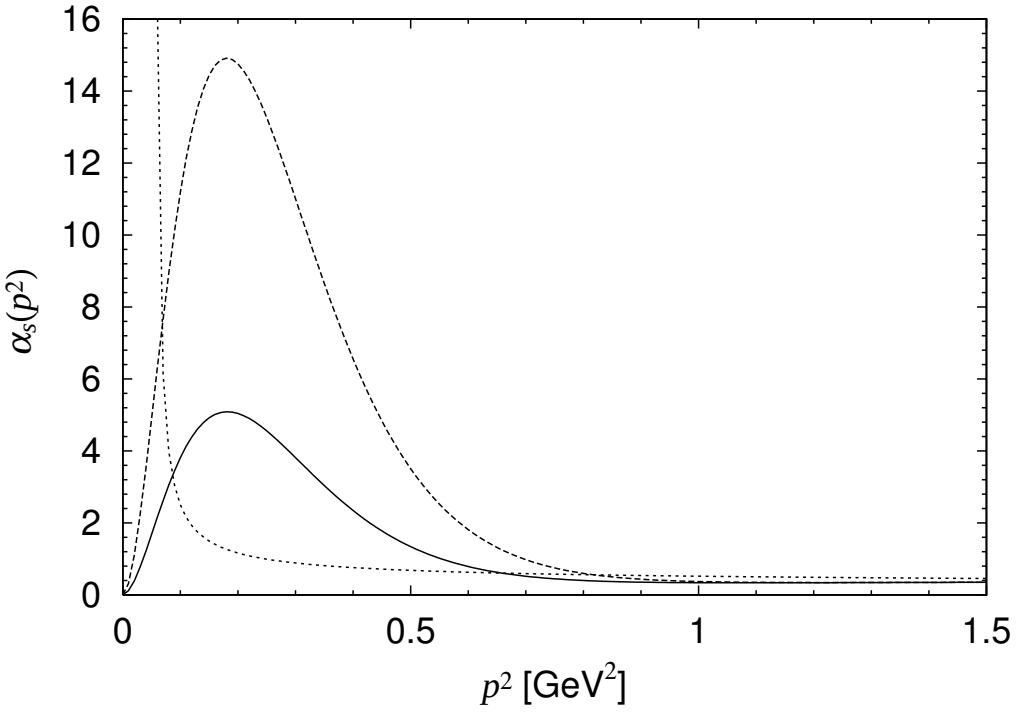

Fig.3